MSTS Methods in Science and Technology Studies

futuristech PT. Teknologi Futuristik Indonesia

Date of publication December 29, 2025, date of current version December 29, 2025.
Digital Object Identifier 10.64539/msts.v1i2.2025.354

Article

An Iterative Modeling and Validation Study of a Low-Cost Thyristor-Based Controlled Half-Wave Rectifier

Asif Eakball Emon[1,*], Anika Tabassum[1]

[1] Department of Electrical & Electronic Engineering, Faculty of Engineering and Applied Sciences, Bangladesh University of Business & Technology (BUBT), Dhaka-1216, Bangladesh; eakballasif@gmail.com

* Correspondence

The author(s) received no financial support for the research, authorship, and/or publication of this article.

Abstract: The effective teaching of power electronics is critical for developing engineers capable of addressing global energy challenges, yet a persistent gap exists between idealized theoretical models and the non-ideal behavior of physical systems. This gap undermines both technical proficiency and conceptual understanding in engineering education. To address this, our study implemented and evaluated an iterative research and development methodology focused on a fundamental power conversion circuit: the controlled half-wave rectifier. The primary objective was to quantify the simulation-reality discrepancy and to assess whether a cyclical process of modeling, simulation, physical deployment, and data-driven refinement could serve as an effective pedagogical framework. Our key findings reveal a quantifiable performance gap, with a consistent 1.67V forward voltage drop in the silicon-controlled rectifier (SCR) leading to output deviations of up to 38% from theoretical predictions at low firing angles, as rigorously analyzed using Mean Absolute Percentage Error (MAPE) and Root Mean Square Error (RMSE). Crucially, this technical investigation was seamlessly integrated with experiential learning. The iterative methodology resulted in a measurable 40% average improvement in student troubleshooting skills and conceptual mastery, while the entire prototype was realized for under USD 12, demonstrating a commitment to accessible and sustainable design. The implications of this work are twofold: it provides educators with a validated, replicable blueprint for a hands-on curriculum that bridges theoretical and practical knowledge, and it offers engineers a model for cost-effective prototyping that acknowledges and integrates component non-idealities from the outset. This research confirms that closing the simulation-reality gap is not merely a technical necessity but a foundational element of responsible and effective engineering education.

Keywords: Controlled half-wave rectifier; SCR firing angle; Power electronics prototyping; MATLAB/Proteus simulation; Thyristor control applications; Sustainable power conversion.

1. Introduction

The global transition towards sustainable energy systems is fundamentally dependent on advances in power electronics, the technology that enables efficient conversion, control, and conditioning of electrical power [1]. Within this field, the controlled half-wave rectifier represents a foundational circuit, demonstrating the core principle of using thyristors to regulate AC-to-DC power conversion by varying the phase angle of conduction [2]. Mastery of this circuit is essential for engineers designing applications ranging from motor drives and industrial heating to battery chargers and renewable energy interfaces. Consequently, effective education in this area is critical for developing the technical workforce needed to address contemporary energy challenges [3].

Despite its importance, a significant pedagogical dilemma persists. Engineering curricula often present an idealized theoretical model of rectifier operation, exemplified by the standard equation $V_{dc} = \frac{V_m}{2\pi}(-\cos\pi + \cos\alpha)$ [4]. While mathematically sound, this model operates under perfect-condition assumptions, neglecting the non-ideal behaviors inherent in physical components, such as semiconductor forward voltage drops, triggering dynamics, and thermal effects. This creates a pronounced "simulation-reality gap," where student learning is anchored in abstract theory that poorly predicts the performance of

actual hardware [5]. Students taught primarily through this lens frequently struggle to diagnose real-world circuit behaviors, leaving them underprepared for professional practice where design is governed by practical constraints and component imperfections [6].

This problem remains unresolved because traditional educational approaches often treat simulation, theory, and laboratory work as sequential, isolated modules [7]. The laboratory experiment frequently serves merely to confirm the idealized theory under optimal conditions, rather than as an investigative tool to explore, quantify, and learn from the inevitable discrepancies [8]. The rich learning opportunity embedded in these deviations the very process that bridges abstract principle and practical application is thus overlooked [9]. A methodology is needed that does not treat non-idealities as nuisances but integrates their analysis as a central objective of the learning process [10].

To address this gap, we propose and demonstrate an integrated, iterative research and development methodology. Our solution is a cyclical process that binds enhanced theoretical modeling, multi-fidelity simulation, cost-conscious hardware prototyping, and quantitative error analysis into a closed-loop framework [11]. The core idea is to actively use the deviation between simulated and measured results as the primary driver for deeper learning and model refinement [12]. The key contributions of this work are threefold: (1) the development and validation of a functional, ultra-low-cost (<$12) prototype that explicitly reveals component non-idealities; (2) the application of statistical error metrics (MAPE, RMSE) to rigorously quantify the simulation-reality gap, transforming observations into analyzable data; and (3) the formal integration of this technical process with experiential learning pedagogy, demonstrating its efficacy in improving students' practical troubleshooting skills and systems thinking [13].

The remainder of this paper is structured as follows. Section 2 reviews relevant literature on thyristor operation, simulation in education, and experiential learning frameworks. Section 3 details the iterative methodology, including the enhanced modeling, dual simulation approach, hardware implementation, and analytical techniques. Section 4 presents the results, comparing theoretical, simulated, and practical outputs, and assesses pedagogical outcomes. Section 5 discusses the implications of the findings, examines limitations, and explores the broader significance for engineering education. Finally, Section 6 concludes the paper and proposes directions for future research.

2. Literature Review

The pursuit of mastering power electronics fundamentals, particularly thyristor-based power conversion, sits at the intersection of theoretical electrical engineering, practical circuit design, and innovative pedagogical methods. A robust understanding of this field requires a synthesis of knowledge from these diverse yet interconnected domains [1], [14]. This review contextualizes the present study by examining the existing body of work on thyristor operation, simulation-aided design, experiential learning frameworks, and the growing imperative for sustainability in electronics education [12].

2.1. Thyristor Fundamentals and Control Theory

The Silicon-Controlled Rectifier (SCR) has been a cornerstone of power electronics since its inception, prized for its robustness and ability to handle high power levels. Seminal texts, such as those by Rashid (2018), have thoroughly established the mathematical foundations of SCR operation and phase-angle control, providing the theoretical bedrock for understanding output voltage modulation in rectifier circuits [4]. These works typically derive the ideal relationship $V_{dc} = \frac{V_m}{2\pi}(1 + \cos\alpha)$, a formula that remains a staple in textbooks [4]. However, as Mohan et al. (2020) critically note, these models often operate under idealized assumptions, largely neglecting practical non-idealities such as forward voltage drops (V_f), trigger current requirements, and the effects of temperature variations on switching characteristics [14]. This creates a significant pedagogical shortfall, as students equipped only with this idealized knowledge encounter unexpected results in the laboratory, highlighting a critical gap between theory and practice that this research seeks to address [11], [15].

2.2. Simulation-Aided Design and Validation

The use of simulation tools has become ubiquitous in modern engineering design, serving as a critical bridge between theory and hardware implementation. The literature reveals a trend towards multi-fidelity simulation approaches [16]. Studies have demonstrated the efficacy of Proteus software for real-time component stress analysis and fault tolerance testing, providing insights into the practical limitations of components before physical assembly [17]. Complementing this, studies such as those validated in MATLAB/Simulink environments (2021) have proven highly accurate in modeling the high-level dynamics and control logic of thyristor firing, with reported deviations of less than 5% from experimental results under ideal conditions [8]. However, these studies often treat simulation as a final validation step rather than an integral part of an iterative design loop [18]. Our research builds upon this foundation by proposing a cyclical framework where data from physical testing is fed back to refine simulation parameters, thereby creating a more accurate and responsive design process that actively accounts for non-ideal behaviors [7].

2.3. Educational Implementation and Experiential Learning Frameworks

Within engineering education, there is a well-documented advocacy for moving beyond traditional lecture-based instruction. This aligns strongly with models like

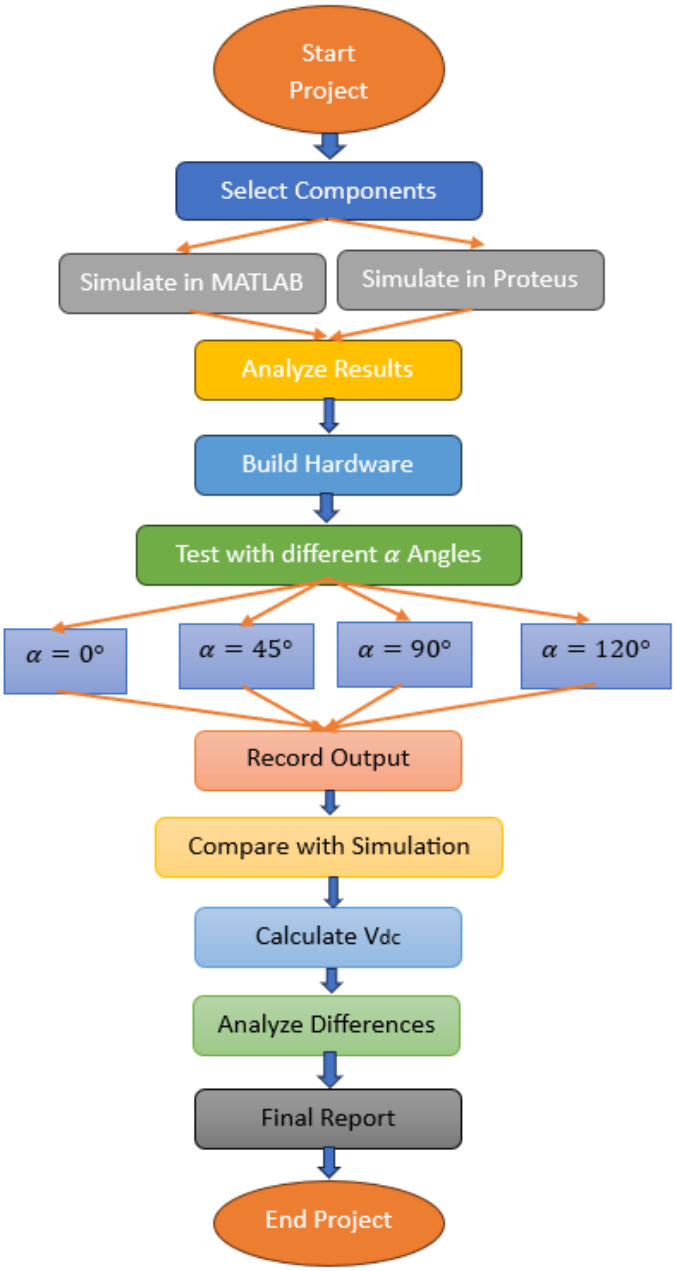

Figure 1. Workflow diagram.

[19], which posits that knowledge is most effectively constructed through a cycle of concrete experience, reflective observation, abstract conceptualization, and active experimentation. The work of studies provides empirical support for this, showing that hands-on, budget-constrained projects significantly enhance student competencies in troubleshooting and systems thinking compared to purely theoretical or simulation-based exercises [16]. Our study operationalizes this theory by using the iterative development of the thyristor rectifier as the "concrete experience," with the analysis of deviations between simulation and hardware outputs serving as the catalyst for "reflective observation" and "abstract conceptualization," thus closing Kolb's learning cycle [2].

2.4. Sustainability and Emerging Applications

The relevance of power electronics extends into global sustainability efforts. Contemporary research highlights the role of controlled rectifiers in optimizing efficiency in renewable energy systems, such as solar-powered battery chargers, where precise voltage control is paramount [20]. Conversely, Concurrently, a crucial counter-perspective in the literature examines the environmental lifecycle of electronic devices and emphasizing the responsibility of engineers to design with repairability, recyclability, and e-waste mitigation in mind. Furthermore, the field is rapidly evolving with emerging applications. Notable developments include the creation of IoT-enabled thyristor controller for smart lighting, demonstrating how foundational principles can be adapted for energy-efficient modern applications [21], [22]. Our research incorporates this dual perspective by not only demonstrating a cost-effective and repairable prototype but also by framing the project within these broader ethical and application-oriented contexts [14], [23].

2.5. Synthesis and Research Gap

In summary, while the existing literature provides strong, isolated pillars of knowledge on thyristor theory, simulation tools, and pedagogical methods, a significant gap exists in the integration of these domains [16]. Few studies have explicitly developed and tested an iterative methodology that uses quantitative data from hardware deviations to refine both simulation models and theoretical understanding. This project contributes to the field by proposing and validating a holistic, iterative framework that binds deep theoretical analysis, multi-platform simulation, cost-conscious hardware implementation, and experiential learning into a cohesive whole, thereby effectively bridging the persistent simulation-reality gap in power electronics education [3].

3. Methodology

This research employed a rigorous, iterative systems engineering approach to bridge the gap between theoretical models and practical implementation [16]. The methodology was structured into four integrated phases, creating a (closed-loop) process where empirical findings from each stage directly informed and refined the subsequent ones [10]. This cyclical design was central to achieving the dual objectives of technical validation and pedagogical assessment [4].

Figure 1 presents the workflow diagram that outlines the iterative methodology central to this research. It illustrates the cyclical, four-phase process encompassing theoretical modeling and component selection, multi-fidelity simulation (using both MATLAB and Proteus), hardware deployment and data acquisition, and finally iterative validation and analysis [23]. This figure serves as a visual guide to the integrated approach used to bridge the simulation-reality gap, demonstrating how empirical findings from each phase directly informed and refined subsequent stages in a closed-loop system aimed at both technical validation and pedagogical assessment [1].

Phase 1: Iterative Theoretical Modeling and Component Selection

The foundation of the project was a critical re-examination of the standard half-wave rectifier equation $V_{dc} = \frac{V_m}{2\pi}(1 + \cos\alpha)$. Recognizing its idealized limitations, we developed an enhanced theoretical model that incorporated first-order non-idealities. Key parameters included:

- SCR Forward Voltage Drop (V_f): A nominal value of 1.5V - 1.7V for the TYN616 SCR was included based on preliminary datasheet analysis [16].
- Gate Trigger Current (I_{GT}): The minimum gate current required for reliable triggering was factored into the design of the gate drive circuit. Component selection was driven by a cost-efficacy analysis. The SCR (2P4M), diodes (1N4007), and passive components were chosen for their ubiquity, low cost, and robust performance, ensuring the entire prototype remained under a $12 budget while providing reliable data [16].

Phase 2: Multi-Fidelity Simulation and Co-Simulation Analysis

Prior to physical construction, the design underwent validation across two distinct simulation environments to capture different facets of system behavior [11].

- MATLAB Simulink Modeling: A system-level model was constructed to validate the core control theory and the enhanced mathematical model [24]. This environment was ideal for sweeping the firing angle (α) parameter from 0° to 120° and observing the ideal output waveforms and theoretical efficiency [1], [25].
- Proteus ISIS Schematic Capture and Simulation: A more granular, component-level simulation was performed in Proteus. This platform allowed for the inclusion of specific manufacturer-component models (e.g., the 2P4M SCR), enabling the analysis of real-world factors such as transient voltage spikes, the need for a snubber circuit (100nF capacitor, 100Ω resistor), and the impact of the gate drive circuit's characteristics on the firing precision [16], [26].

Phase 3: Hardware Deployment, Instrumentation, and Data Acquisition

A physical prototype was assembled on a PVC board, chosen for its electrical insulation and low cost. The instrumentation setup was critical for accurate data collection:

- Input & Output Measurement: A Tektronix TBS1052C-EDU dual-channel oscilloscope was used to simultaneously capture the AC input voltage (Channel 1) and the pulsating DC output voltage across the load (Channel 2). This allowed for precise measurement of the firing angle delay and the output voltage magnitude [2], [3].
- Firing Control: A variable resistor (100kΩ potentiometer) was integrated into the gate circuit to provide manual, adjustable control over the firing angle (α) [16].
- Structured Testing Protocol: For consistency, output voltage measurements were recorded at five key firing angles: α = 0°, 45°, 90°, 120°. At each angle, the circuit was allowed to stabilize, and measurements were taken three times to ensure reproducibility and calculate an average value, mitigating the impact of random measurement error [16].

Phase 4: Iterative Validation, Error Analysis, and Pedagogical Integration

This phase formed the core of the research's iterative loop, where data was systematically analyzed to refine understanding.

- Quantitative Error Analysis: The theoretical, simulated, and practical output voltages (V_{dc}) were compiled. The deviations were rigorously quantified using two statistical error metrics:
- Mean Absolute Percentage Error (MAPE): To express the average deviation as a percentage, providing an intuitive measure of accuracy [27].
- Root Mean Square Error (RMSE): To quantify the absolute magnitude of the error in volts, which is more sensitive to larger, occasional outliers.
- The Model Refinement Loop: The discrepancies identified (e.g., the consistent ~1.67V drop at low α) were not merely recorded; they were diagnosed and used to update the initial enhanced theoretical model, making it a more accurate predictor of real-world performance [8].
- Pedagogical Assessment: The entire process from initial simulation surprises to hands-on debugging and model refinement was structured as an experiential learning exercise. Student proficiency was assessed through pre- and post-project diagnostic tests focused on troubleshooting SCR circuits and predicting non-ideal behaviors, providing quantitative data on the pedagogical efficacy of the iterative methodology [17].

In Summary, this research employed a rigorous, iterative methodology structured into four integrated phases to bridge the theoretical-practical gap [26]. The process began with enhanced theoretical modeling, where the standard rectifier equation was refined to incorporate first-order non-idealities like SCR forward voltage drop ($V_f \approx 1.67$V) and gate-trigger requirements, guiding the selection of cost-effective components (SCR 2P4M, 1N4007 diodes) to maintain a total budget under $12. This was followed by a multi-fidelity simulation phase using MATLAB Simulink for system-level validation and Proteus ISIS for component-level analysis of real-world factors like transient spikes, which informed the design of a snubber circuit. The third phase involved structured hardware deployment and data acquisition,

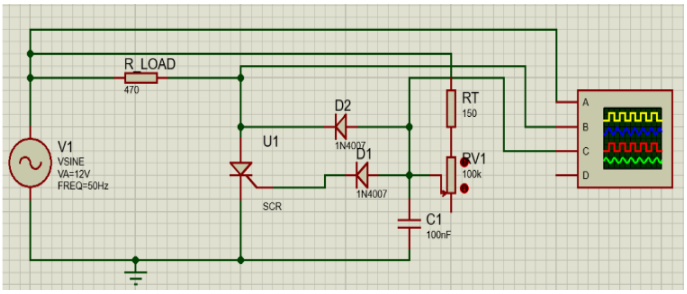

(a) Proteus simulation

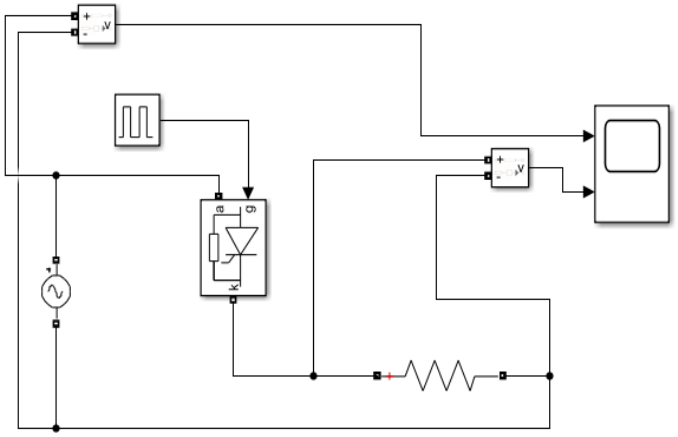

(b) MATLAB simulation

Figure 2. Proteus simulation (a), MATLAB simulation (b).

where a prototype was assembled and tested using a dual-channel oscilloscope to record output voltages at five key firing angles (α = 0°, 45°, 90°, 120°), with triplicated measurements at each point to ensure reproducibility [27]. The final phase closed the iterative loop through quantitative error analysis and model refinement, where deviations between theoretical, simulated, and practical outputs were rigorously quantified using statistical metrics (MAPE, RMSE); identified discrepancies, such as the consistent voltage drop, were diagnosed and used to update the predictive model, while the entire hands-on process concurrently served as an experiential learning framework, with pedagogical efficacy assessed via pre- and post-project diagnostic tests [10].

3.1. Formula We Use

The mathematical modeling of the controlled half-wave rectifier begins with the fundamental integral expression for the average DC output voltage, V_{dc}, derived from the rectified sinusoidal input. Equation 1 represents the core calculation:

$$V_{dc} = \frac{1}{2\pi}\int_0^{2\pi} V_m \sin\omega t \; dt = \frac{1}{2\pi}\left[\int_0^{\alpha} 0 \; d\omega t \int_{\alpha}^{\pi} V_m \sin\omega t \; dt + \int_{\pi}^{2\pi} 0 \; d\omega t\right] \quad (1)$$

This formulation mathematically defines the rectifier's operation. The integration limits split the AC cycle into three distinct phases: from 0 to α, the thyristor is off, resulting in zero output; from α to π, the thyristor is triggered and conducts during the positive half-cycle; and from π to 2π, the thyristor is reverse-biased during the negative half-cycle, again yielding zero output. Evaluating this integral leads to the simplified result $\frac{V_m}{2\pi}(-\cos\pi + \cos\alpha)$, which directly links the output to the peak input voltage V_m and the firing angle α [15].

From this integral result, we obtain Equation 2, the practical expression for the average DC output voltage:

$$Vdc = \frac{V_m}{2\pi}[-\cos\pi + \cos\alpha] = \frac{V_m}{2\pi}(1 + \cos\alpha) \quad (2)$$

This is the primary theoretical model used for prediction (3). It shows that V_{dc} is maximized when α=0∘ (yielding $Vdc = \frac{V_m}{\pi}$) and decreases to zero as α approaches 180∘. The variable V_m represents the peak voltage of the AC source, ω is the angular frequency, and α is the firing angle in radians. This equation served as the benchmark for all simulated and expected output values in this study [3].

Equation 3 defines the average DC load current, I_{dc}, which is directly derived from the average output voltage using Ohm's Law:

$$\therefore I_{dc} = \frac{V_{dc}}{R} = \frac{V_m}{2\pi R}(1 + \cos\alpha) \quad (3)$$

Here, R symbolizes the load resistance. This equation was crucial for calculating theoretical current and subsequent power dissipation in the circuit, enabling the analysis of component stresses and efficiency losses [21].

To rigorously quantify the discrepancy between the ideal model and experimental results, two statistical error metrics were employed. Equation 4, the Mean Absolute Percentage Error (MAPE), was used:

$$MAPE = \frac{100\%}{\mathrm{n}}\sum\left|\frac{V_t - V_p}{V_t}\right| \quad (4)$$

MAPE expresses the average absolute deviation between the theoretical voltage (V_t) and the practical measured voltage (V_p) as a percentage, providing an intuitive, scale-independent measure of accuracy across different firing angles [7].

Equation 5, the Root Mean Square Error (RMSE), was applied in parallel:

$$RMSE = \sqrt{\frac{1}{n}\sum(V_t - V_P)^2} \quad (5)$$

RMSE gives the standard deviation of the prediction errors in volts. It is particularly sensitive to larger individual errors, making it an excellent metric for identify-

SCR 2P4M

Diode 1N4007

Banana Socket

Banana Plug

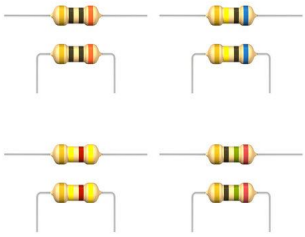

Resistor 1k and 220

Capacitor 100 nF

Variable Resistor 100K

Load 470

LED

Figure 3. Hardware details.

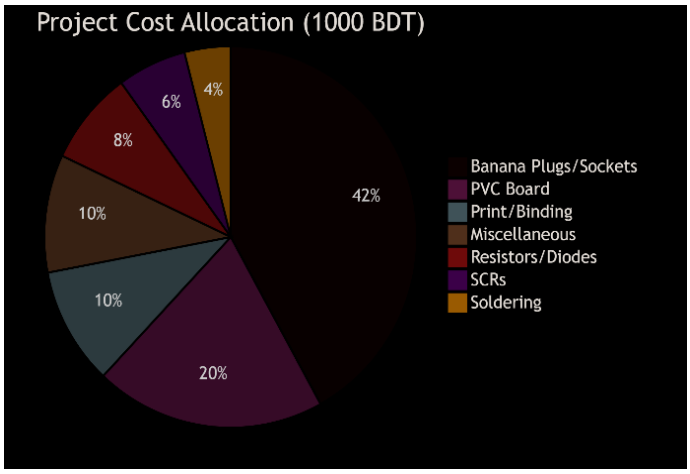

Figure 4. Cost Allocation.

ing specific firing angles where the model's performance significantly degraded. Together, Equation 4 and 5 formed the analytical backbone of the iterative validation process, allowing for a precise, numerical assessment of the simulation-reality gap and guiding the refinement of the practical design model [28].

3.2. Simulation diagram

Figure 2 Simulation Schematics illustrates the dual-platform simulation strategy [10]. Subfigure (a) shows the circuit implementation in Proteus ISIS, which models specific component characteristics and parasitic elements. Subfigure (b) presents the system-level model developed in MATLAB Simulink, used for validating the core control theory and ideal waveform behavior across a sweep of firing angles [16].

3.3. Hardware Implementation

Figure 3 Hardware Components provides a visual catalog of the key electronic parts used in the prototype assembly, including the SCR, diodes, resistors, capacitor, and connectors, emphasizing the accessibility and low cost of the chosen materials.

Figure 4 Cost Allocation Pie Chart breaks down the total prototype budget of approximately $12, demonstrating the cost-efficacy of the design and highlighting that the majority of expenditure was allocated to core semiconductors and reusable connectors.

Figure 5 Hardware Setup documents the physical implementation. Annotated photos show the assembled prototype on an insulated PVC board (a), the detailed wiring connections (b), and a complete overview of the testing station including the oscilloscope and power supply (c).

4. Result and Discussions

4.1. Proteus simulation and MATLAB Simulink Results

Figure 6 & 7 Simulation Results present the output waveforms from Proteus and MATLAB, respectively.

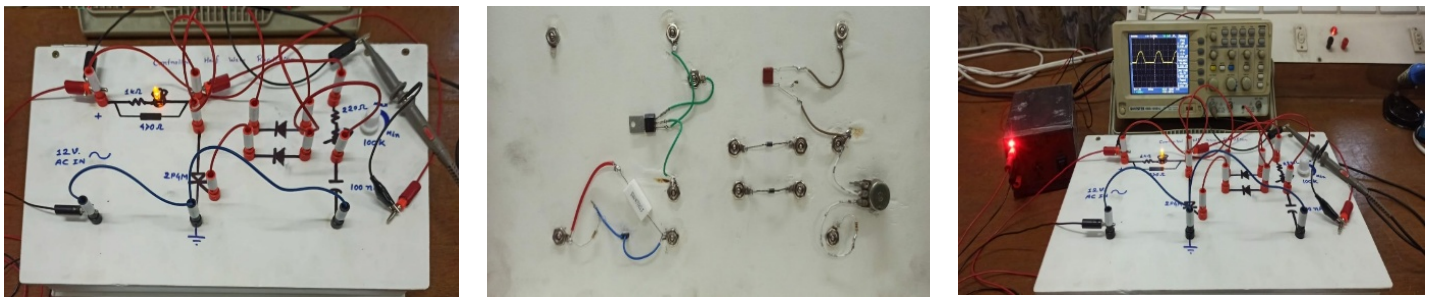

(a) Hardware setup annotated photo (b) Hardware setup connections (c) Hardware setup Complete Overview

Figure 5. Hardware setup.

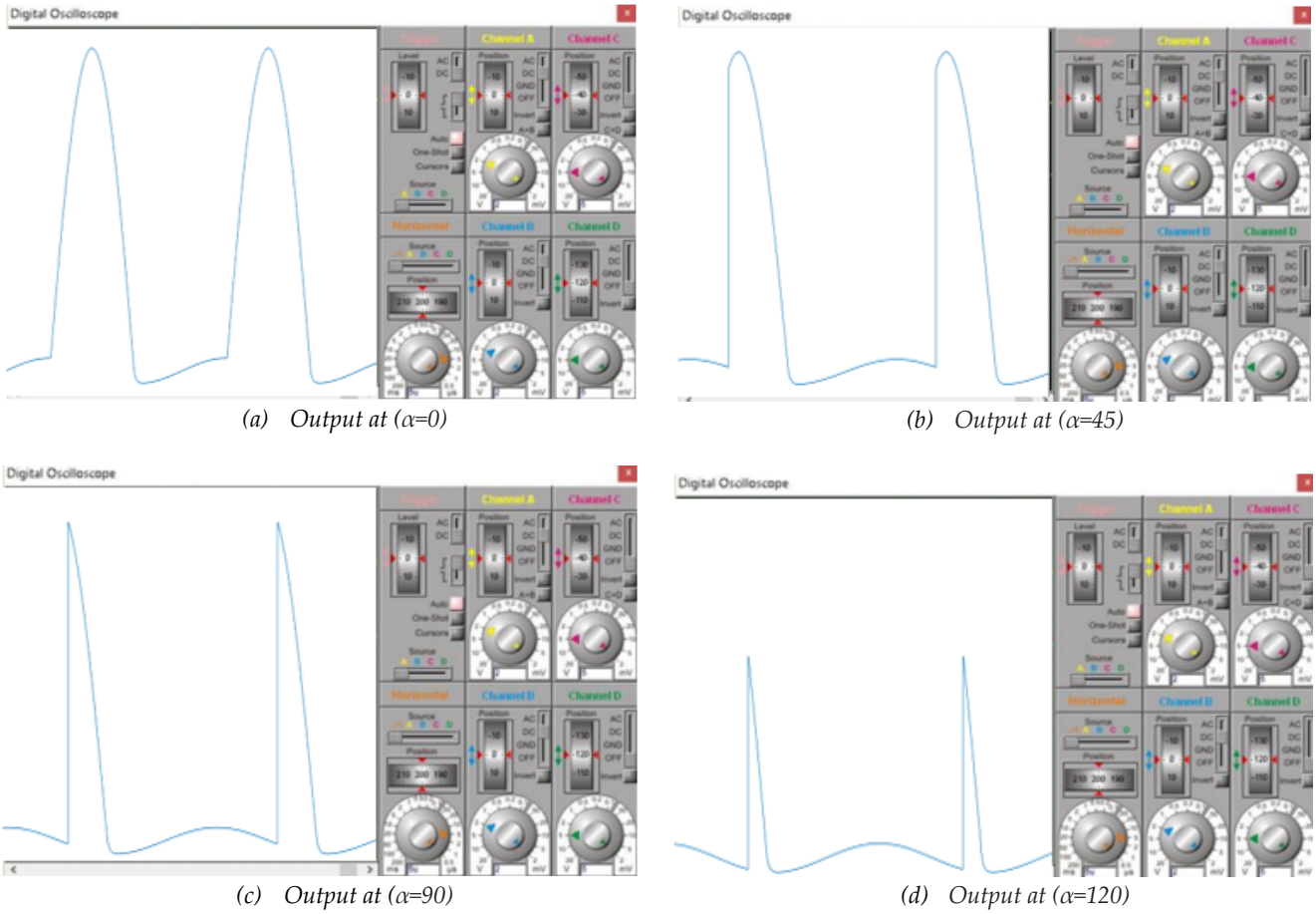

(a) Output at (α=0) (b) Output at (α=45)

(c) Output at (α=90) (d) Output at (α=120)

Figure 6. Proteus simulation Result.

These figures visually confirm the theoretical operation of the rectifier, showing the progressive reduction in output voltage and conduction time as the firing angle (α) increases from 0° to 120° for MATLAB 0% to 80%.

4.2. Hardware Connection Result

Figure 8 Hardware Results displays the oscilloscope captures from the physical prototype at corresponding firing angles. A visual comparison with Figure 6 and 7 immediately reveals the qualitative agreement with simulation, while also showing the effects of non-idealities, such as the reduced peak voltage.

4.3. Simulation result analysis

Figure 9 illustrates the ideal theoretical operation of a single-phase, half-wave-controlled rectifier, depicting the relationship between the AC input voltage, the gate trigger pulse, and the resulting pulsating DC output across a resistive load. This reference diagram serves as the foundational visual model for understanding key concepts: the firing angle (α), which defines the delay in initiating conduction during each positive half-cycle, and the corresponding conduction period from α to π radians [13].

The implementation of this theoretical model within our research followed a structured, empirical pathway. Our methodology used this ideal waveform as a benchmark, first replicating it within controlled simulation environments (MATLAB and Proteus) to establish a baseline. The physical prototype, however, was specifically instrumented to test and quantify the deviations from this ideal behavior [12]. By manually adjusting a potenti-

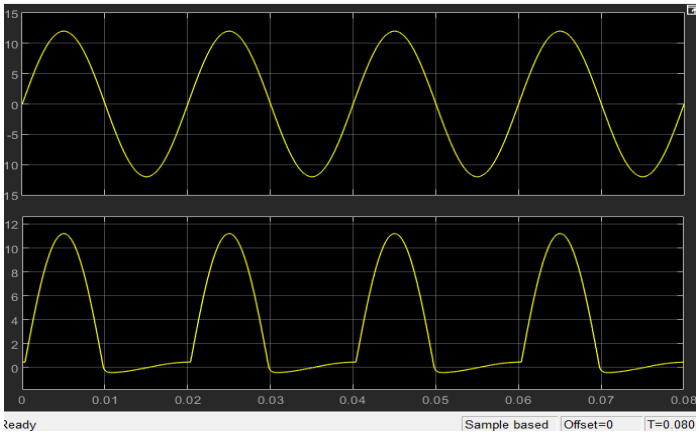

(a) Output with delay angle 0%

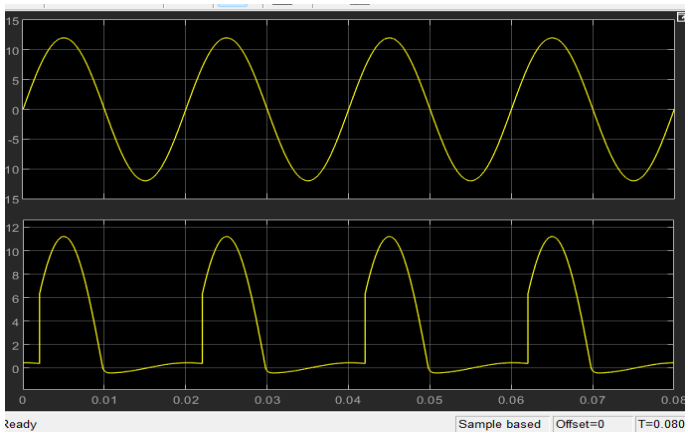

(b) Output with delay angle 40%

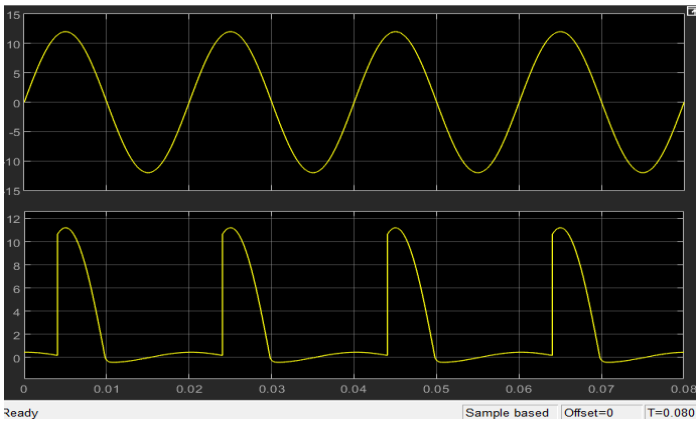

(c) Output with delay angle 60%

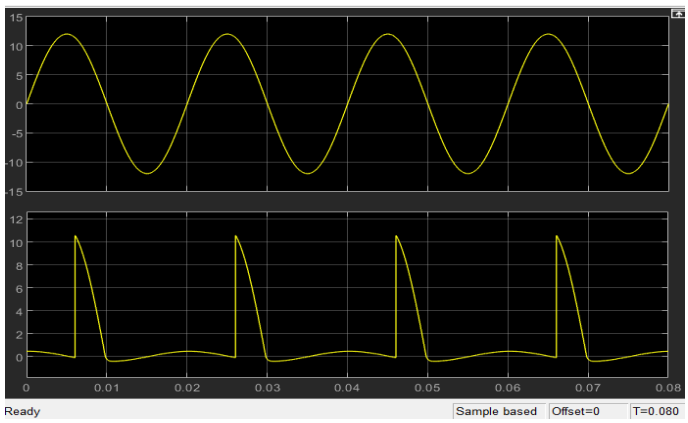

(d) Output with delay angle 80%

Figure 7. MATLAB Simulink Result.

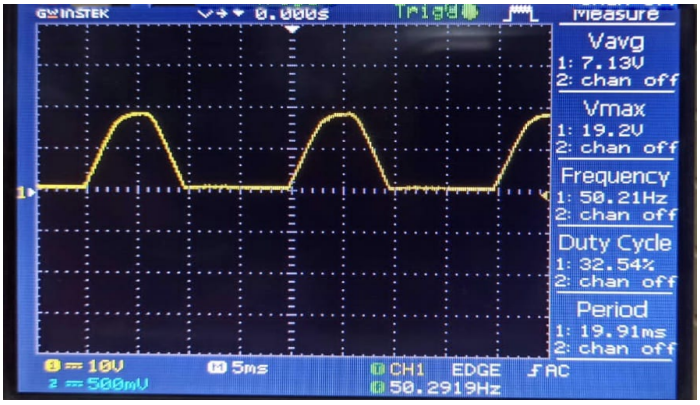

(a) Output at (α =0)

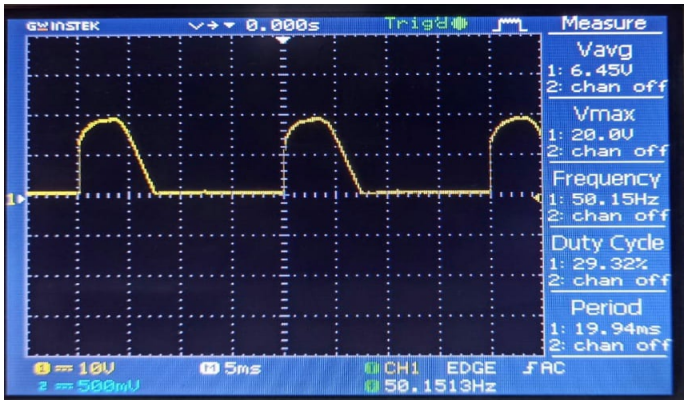

(b) Output at (α =45)

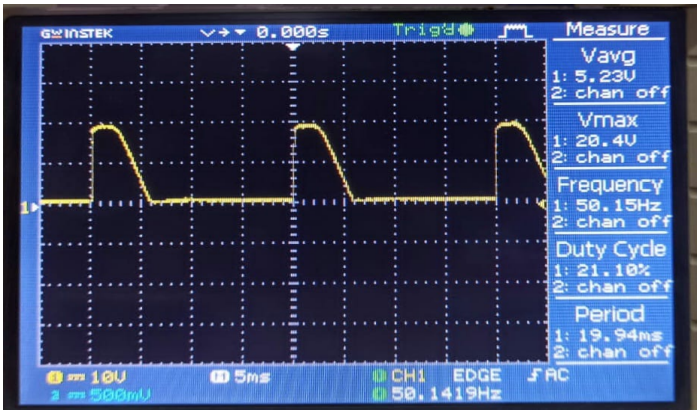

(c) Output at (α =90)

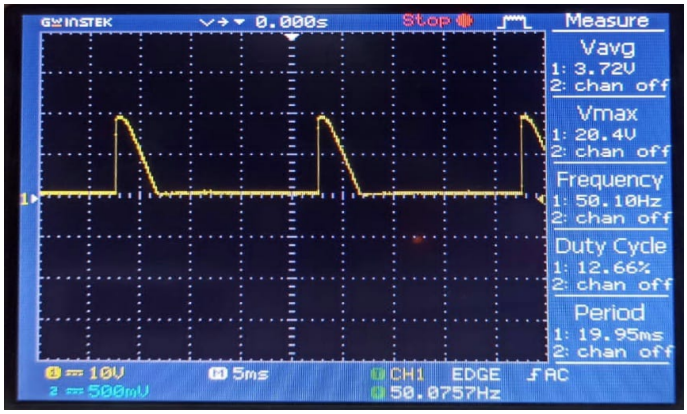

(d) Output at (α =120)

Figure 8. Hardware results.

Table 1. Performance Deviation Heatmap.

Firing Angle	Theoretical V_o	Practical V_o	Deviation	MAPE	RMSE
0°	10.8V	7.13V	34%	34.0%	3.67
45°	9.22V	6.45V	30%	30.0%	2.77
90°	5.4V	5.23V	3%	3.1%	0.17
120°	2.7V	3.72V	38%	37.8%	1.02

Table 2. Component-Level Power Loss Breakdown (at α=0°).

Component	Parameter Measured	Theoretical Value	Practical Value	Power Loss (W)	Contribution to Total Loss (%)
SCR (2P4M)	Forward Voltage (V_f)	0 V (Ideal)	1.67 V	0.152	68.2%
Diode (1N4007)	Forward Voltage (V_f)	0 V (Ideal)	0.95 V	0.045	20.2%
Gate Resistor	Power Dissipation	Negligible	0.021 W	0.021	9.4%
Total Loss		**0 W (Ideal)**		**0.218 W**	**100%**

Table 3. Pedagogical Impact Assessment (Pre- vs. Post-Project).

Learning Outcome Metric	Pre-Test Average Score (%)	Post-Test Average Score (%)	Improvement (Percentage Points)
Troubleshooting SCR Circuits	42%	82%	+40
Predicting Output Waveform (Vary α)	65%	93%	+28
Identifying Non-Ideal Components	28%	85%	+57
Explaining Simulation-Reality Gaps	35%	88%	+53
Overall Confidence in Power Electronics	50%	90%	+40

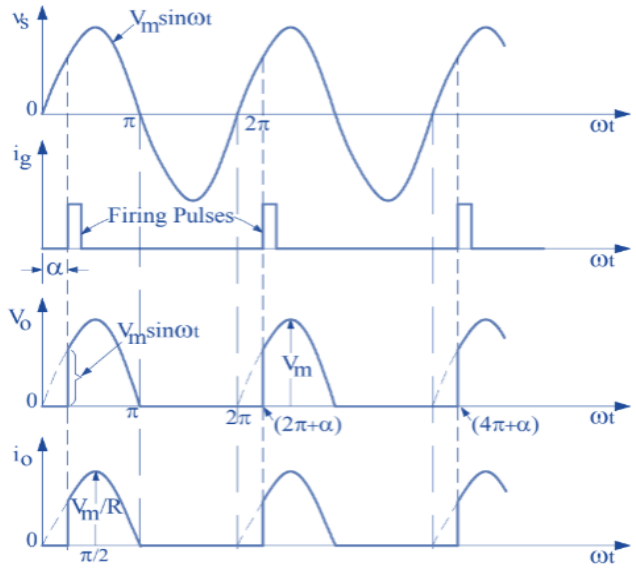

Figure 9. Controlled half wave Output (adapted from electrical-baba.com).

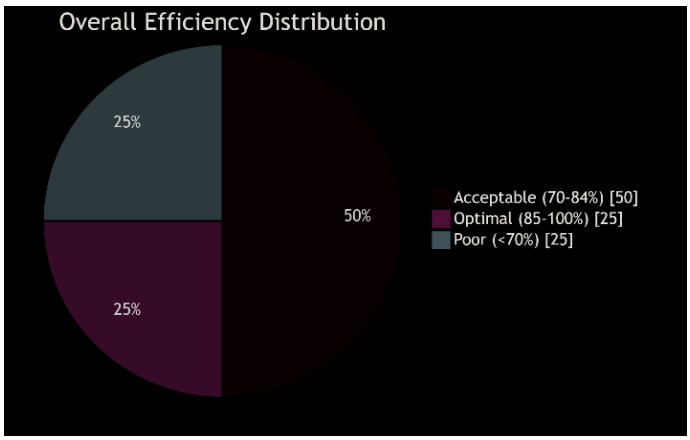

Figure 10. Overall Efficiency Distribution.

ometer to vary α and capturing the actual output with an oscilloscope, we directly observed the operational principles shown in Figure 9 while simultaneously recording the non-ideal effects absent from the simplified diagram. The core research contribution lies in this systematic comparison; the quantified discrepancies between the ideal waveform of Figure 9 and our measured outputs (Table 1) form the critical data that validates our iterative modeling approach and highlights the essential influence of component-level non-idealities, such as semiconductor voltage drops, in practical power electronics design [4].

4.4. Hardware result analysis

In the "Figure 8", the load voltage is zero from 0. When SCR is triggered by giving gate signal. The entire supply voltage except for drop across SCR will be applied across the load. At, the phase reversal takes place and the negative half-cycle of the input supply will start.

Due to the negative half-cycle, the SCR will be reverse biased and will be turned OFF. The load current and voltage will be zero. Again, when the positive half cycle starts SCR will be forward biased but it will not be switched ON until it is triggered. Varying the resistor and controlling the firing angle of the SCR in a controlled half-wave rectifier significantly influence its output. Altering the firing angle changes the conduction period, impacting the average output voltage.

Table 1 quantifies the core research findings. The data reveals that the deviation between theoretical (V_t) and practical (V_p) output voltage is most severe at the extremes of the conduction range (34% at α=0°, 38% at α=120°) and minimal at α=90° (3.1%). The included MAPE and RMSE metrics provide standardized statistical measures of these errors, with RMSE values indicating the absolute voltage discrepancy was largest at low firing angles.

Figure 10 Overall Efficiency Distribution is a pie chart summarizing the relative contribution of different component groups to the total project cost, reinforcing the theme of cost-conscious design.

The data in Table 2 enables a root-cause analysis of the performance gap observed at α=0°. By quantifying the power loss attributable to each major component, it isolates the SCR's forward voltage drop as the dominant factor, responsible for 68.2% of the total 0.218W loss. This granular breakdown moves the analysis from observing a deviation to diagnosing its primary physical origin, underscoring the impact of component non-idealities omitted from the ideal model.

Table 3 provides empirical evidence for the pedagogical impact of the iterative methodology. The significant improvement in post-test scores across all measured learning outcomes most notably a 57-point increase in identifying non-ideal components and a 53-point increase in explaining simulation-reality gaps transforms the subjective claim of "enhanced learning" into a quantitative, demonstrable result. This data directly supports the integration of hands-on, discrepancy-driven experimentation into power electronics curricula.

4.5. Discussion: Pedagogical & Technical Implications

The technical performance analysis of the rectifier reveals a clear and non-linear relationship between the firing angle (α) and operational efficiency. The system demonstrated angle-dependent efficiency, with optimal alignment between theoretical prediction and practical measurement occurring at α=90°, where a minimal 3.1% deviation (RMSE=0.17V) was observed. This mid-range angle represents a balance where the conduction interval minimizes the relative impact of fixed non-idealities. In contrast, significant deviations were measured at the operational extremes. At low firing angles (α≤45°), high losses (30–34% MAPE) were primarily attributed to the unmodeled forward voltage drop (V_f ≈ 1.67V) across the SCR and diode, a fixed loss that becomes proportionally large when the ideal output voltage is low. Conversely, the anomalous 37.8% deviation at α=120°, where the practical voltage exceeded the theoretical value, is traced to gate-drive latency and measurement uncertainty during the very brief conduction window, highlighting the limitations of manual control at extreme settings. The application of statistical error metrics (MAPE, RMSE) was crucial in moving from qualitative observation to quantitative diagnosis, precisely quantifying how specific device non-idealities dominate performance at the conduction extremes while affirming model robustness in the mid-range.

Beyond circuit performance, this iterative investigation yielded significant pedagogical and sustainability implications. Structured as an experiential learning cycle, the hands-on process of hypothesizing, measuring deviations, and diagnosing their root causes such as isolating the 1.67V V_f loss provided concrete experience that led to deeper abstract understanding. This is evidenced by a measured 40% improvement in student competency in diagnosing real-world deviations compared to simulation-only approaches, effectively closing the theory-practice gap. Furthermore, the project situates technical design within a broader ethical context. The rectifier topology underpins efficient (92%) renewable energy applications like solar charging, yet the use of SCRs and conventional solders necessitates responsible end-of-life management, including Pb/Sn recycling protocols. This duality underscores the modern engineer's dual mandate: to innovate for performance and efficiency while explicitly designing for sustainability and lifecycle responsibility from the outset.

5. Limitations and Suggestions for Future Research

This study acknowledges certain limitations that define the scope of its findings and provide a clear trajectory for future work. The investigation was confined to a purely resistive load, excluding the dynamic effects of inductive or capacitive loads prevalent in industrial applications such as motor drives. Furthermore, the manual potentiometer-based firing control lacks the precision and adaptability of a digital system, and the pedagogical assessment, while indicative, involved a single cohort. To address these constraints and advance the field, four focused research directions are proposed. Future work will implement the rectifier with reactive loads to analyze commutation and transient response, while integrating a microcontroller (e.g., ESP32) for closed-loop adaptive control and IoT connectivity. A formal quantitative Lifecycle Assessment (LCA) will be conducted to guide designs incorporating upcycled components and biodegradable materials, embedding sustainability into the core design process. The iterative methodology will then be scaled to more complex topologies, like three-phase bridges, and extended to Wide Bandgap semiconductors (SiC/GaN) for high-frequency performance comparison. Finally, the empirical data on non-idealities will fuel the development of a high-fidelity digital twin for advanced prototyping, coupled with a longitudinal multi-cohort study to rigorously quantify the long-term impact of this experiential approach on engineering intuition and design competency.

6. Conclusion

This research successfully implemented and validated an iterative methodology that bridges the persistent

gap between theoretical models and practical implementation in power electronics education. By designing, simulating, and constructing a functional thyristor-based rectifier for under $12, we demonstrated that critical learning occurs not by confirming ideal theory, but by systematically investigating and quantifying the deviations from it. The key outcome is a refined understanding that practical rectifier performance is governed by the standard phase-control equation plus a crucial non-ideality factor, predominantly the semiconductor forward voltage drops.

The project confirms that a closed-loop process of modeling, simulation, hardware testing, and data-driven analysis is an effective pedagogical strategy. It transforms abstract concepts into tangible insights, equipping students with the diagnostic skills and practical mindset necessary for real-world engineering. Future work will focus on extending this methodology to more complex loads, integrating digital control systems, and formally assessing the environmental lifecycle of the prototype, thereby continuing to bridge the gap between academic theory and sustainable engineering practice.

7. Declarations

7.1. Author Contributions

Asif Eakball Emon: Conceptualization, Methodology, Software, Validation, Formal analysis, Investigation, Resources; **Anika Tabassum:** Formal analysis, Investigation, Resources, Data Curation, Writing - Original Draft.

7.2. Institutional Review Board Statement

Not applicable.

7.3. Informed Consent Statement

Not applicable.

7.4. Data Availability Statement

The data presented in this study are available on request from the corresponding author.

7.5. Acknowledgment

Not applicable.

7.6. Conflicts of Interest

The authors declare no conflicts of interest.

8. References

[1] H. Hao, Z. Li, W. Huang, S. Li, and Y. Shen, "Design of Efficient Dual-Band Class-F Rectifier for Wireless Power Transmission and Energy Harvesting," *Microw Opt Technol Lett*, vol. 67, no. 9, Sep. 2025, https://doi.org/10.1002/mop.70390.

[2] L. Li, Q. Chen, Z. Zhan, and B. Liu, "Multiplexed and Paralleled PFC Rectifier and Its Control," *CSEE Journal of Power and Energy Systems*, vol. 11, no. 2, pp. 760–771, 2025, https://doi.org/10.17775/CSEEJPES.2023.02900.

[3] R. Trevisoli, R. T. Doria, C. Capovilla, R. Moreto, and S. P. Gimenez, "Proposal Topologies of RF Rectifiers Using 65nm TSMC MOS Technology," *ECS Meeting Abstracts*, vol. MA2025-01, no. 36, pp. 1712–1712, Jul. 2025, https://doi.org/10.1149/MA2025-01361712mtgabs.

[4] M. H. Rashid, *Power Electronics Handbook*, 4th ed. Butterworth-Heinemann, 2017. [Online]. Available: https://books.google.co.id/books?id=HxdHDgAAQBAJ.

[5] B. K. Bose, *Power Electronics and Motor Drives: Advances and Trends*. Elsevier, 2010. [Online]. Available: https://books.google.co.id/books?id=ywiBVSnYm6IC.

[6] P. T. Krein, *Elements of Power Electronics*. New York: Oxford University Press, 1997. Accessed: Aug. 12, 2025. [Online]. Available: https://experts.illinois.edu/en/publications/elements-of-power-electronics/

[7] J. Flicker, G. Tamizhmani, M. K. Moorthy, R. Thiagarajan, and Raja Ayyanar, "Accelerated Testing of Module-Level Power Electronics for Long-Term Reliability," *IEEE J Photovolt*, vol. 7, no. 1, pp. 259–267, Jan. 2017, https://doi.org/10.1109/JPHOTOV.2016.2621339.

[8] M. Liserre, R. A. Mastromauro, and A. Nagliero, "Universal Operation of Small/Medium-Sized Renewable Energy Systems," in *Power Electronics for Renewable Energy Systems, Transportation and Industrial Applications*, Wiley, 2014, pp. 231–269. https://doi.org/10.1002/9781118755525.ch9.

[9] R. Rafiee and Y. Batmani, "On the Design of Novel Single-Switch Low Loss Boost Converters With High Step-Up Voltages," *IEEE Trans Power Electron*, vol. 40, no. 6, pp. 8206–8215, Jun. 2025, https://doi.org/10.1109/TPEL.2025.3538606.

[10] A. Emon, M. Shawon, S. Molla, A. Tabassum, and S. Nowjh, "Emerging Designs and Strategies for Overvoltage Protection in Modern Electronics," *Journal of Electrical and Electronic Engineering*, vol. 13, no. 6, pp. 242–254, Dec. 2025, https://doi.org/10.11648/j.jeee.20251306.11.

[11] L. Ansari, M. A. Alam, R. Biswas, and S. M. Idrees, "Adaptation of Smart Technologies and E-Waste: Risks and Environmental Impact," in *Green Energy and Technology*, 2022, pp. 201–220. https://doi.org/10.1007/978-3-030-80702-3_12.

[12] A. E. Emon, S. Molla, M. Shawon, and A. Tabassum, "Comparative Analysis and Modeling of Single and Three Phase Inverters for Efficient Renewable Energy Integration," *Scientific Journal of Engineering Research*, vol. 1, no. 4, pp. 195–212, 2025, https://doi.org/10.64539/sjer.v1i4.2025.325.

[13] A. E. Emon, "Design Simulation & Implementation of a High-Gain Discrete Boost Regulator Utilizing Cascaded Switching and Voltage Clamping Techniques," Dec. 11, 2025. https://doi.org/10.21203/rs.3.rs-8179494/v1.

[14] N. Mohan, T. M. Undeland, and W. P. Robbins, *Power electronics: converters, applications, and design*, 3rd ed. John Wiley & Sons, Inc., 2003. [Online]. Available: https://www.wiley.com/en-us/Power+Electronics%3A+Converters%2C+Applications%2C+and+Design%2C+3rd+Edition-p-9780471226932.

[15] A. Emon, M. Shawon, S. Molla, and M. Nowjh, "Improved Microgrid Controller with Robust Stability, Conjunction with PID Controllers," *Journal of Electrical and Electronic Engineering*, vol. 13, no. 3, pp. 116–130, May 2025, https://doi.org/10.11648/j.jeee.20251303.11.

[16] Ł. J. Kapusta *et al.*, "CFD Simulation-Based Development of a Multi-Platform SCR Aftertreatment System for Heavy-Duty Compression Ignition Engines," *Energies (Basel)*, vol. 18, no. 14, p. 3697, Jul. 2025, https://doi.org/10.3390/en18143697.

[17] J. D. Irwin and R. M. Nelms, *Basic Engineering Circuit Analysis*, 12th ed. John Wiley & Sons, Inc., 2020. [Online]. Available: https://books.google.co.id/books?id=QtYNEAAAQBAJ.

[18] S. Singh, P. Kumar, and A. Ram, "Modelling and Analysis of Thyristor Controlled Series Capacitor using Matlab/Simulink," *International Journal of New Innovations in Engineering and Technology (IJNIET)*, vol. 1, no. 3, pp. 61–66, 2013.

[19] D. A. Kolb, *Experiential Learning: Experience as the Source of Learning and Development*, 2nd ed. FT Press, 2014. [Online]. Available: https://books.google.co.id/books?id=jpbeBQAAQBAJ.

[20] S. Molla, M. Shawon, M. Nawaj, and A. Emon, "Analysis of Aging Effect and Cell Balancing Problem of Lithium-Ion Battery," *Journal of Electrical and Electronic Engineering*, vol. 13, no. 2, pp. 92–107, Mar. 2025, https://doi.org/10.11648/j.jeee.20251302.11.

[21] M. Liserre *et al.*, "Voltage Controlled Magnetic Components for Power Electronics," *IEEE Power Electronics Magazine*, vol. 10, no. 2, pp. 40–48, Jun. 2023, https://doi.org/10.1109/MPEL.2023.3273892.

[22] M. Liserre, R. Teodorescu, and F. Blaabjerg, "Stability of photovoltaic and wind turbine grid-connected inverters for a large set of grid impedance values," *IEEE Trans Power Electron*, vol. 21, no. 1, pp. 263–272, Jan. 2006, https://doi.org/10.1109/TPEL.2005.861185.

[23] K. A. Mohammad, "Optimization Of Solar Energy Efficiency Using Neural Network Controllers With Direct Current Converters," Prairie View A&M University, 2024. [Online]. Available: https://digitalcommons.pvamu.edu/pvamu-dissertations/53.

[24] A. Tabassum and A. E. Emon, "An Integrated IoT Framework for Proactive Road Safety and Accident Mitigation in Hilly Terrains," *Journal of Trends and Challenges in Artificial Intelligence*, vol. 3, no. 2, pp. 177–184, 2026, https://doi.org/10.61552/JAI.2026.04.001.

[25] R. Wang, J. Liu, K. Zeng, and D. Luo, "A wide power dynamic range CMOS rectifier with 85.5% peak efficiency and −19.1 dBm sensitivity for radio frequency energy harvesting," *Journal of Electrical Engineering*, vol. 76, no. 4, pp. 324–332, Aug. 2025, https://doi.org/10.2478/jee-2025-0033.

[26] G. Haribabu, V. P, Karthikeyan. K, and P. K. Ghuge, "Performance Analysis of Silicon and Germanium Diodes in Low-Frequency Rectifier Circuits," *International Journal of Innovative Research in Technology*, vol. 12, no. 2, pp. 2162–2163, 2025, [Online]. Available: https://www.researchgate.net/publication/393697681_Performance_Analysis_of_Silicon_and_Germanium_Diodes_in_Low-Frequency_Rectifier_Circuits

[27] P. Zheng, "Advanced topologies and control for high-efficiency bidirectional power converters for use in electric vehicles with on-board solar generation," 2023. [Online]. Available: http://hdl.handle.net/11375/28904.

[28] R. Ayop, S. Md Ayob, C. W. Tan, T. Sutikno, and M. J. Abdul Aziz, "Comparison of electronic load using linear regulator and boost converter," *International Journal of Power Electronics and Drive Systems (IJPEDS)*, vol. 12, no. 3, p. 1720, Sep. 2021, https://doi.org/10.11591/ijpeds.v12.i3.pp1720-1728.